

LOCAL AND GLOBAL FRICTION FACTOR IN A CHANNEL WITH V-SHAPED BOTTOM

Mirali Mohammadi*

Department of Civil Engineering, Faculty of Engineering
Islamic Azad University, Khoy Branch, Khoy, Iran
m.mohammadi@mail.urmia.ac.ir

*Corresponding Author

(Received: June 13, 2007 – Accepted in Revised Form: May 9, 2008)

Abstract This paper presents an experimental research on the distribution of local friction factor, f_b , and global friction factor, f , over the cross-section of a channel with V-shaped bottom, which typically occurs in sewers and culverts. Several series of experiments were conducted for measuring velocity and boundary shear stress. It is found that, Darcy-Weisbach, f , is more sensitive than other resistance coefficients such as Manning, n . Local boundary shear stress around wet perimeter, τ_b , and depth-averaged velocity, U_d , data are used to evaluate f_b . The results illustrate that, the friction factor is shown to be a function of flow depth as well as being dependent upon the Froude number, Fr . Therefore, the local friction factor does not remain constant across the channel. Meanwhile, the common technique of assuming a constant friction factor over the entire section of the channel has been found to have theoretical justification. The results indicate that the global friction factor decreases as flow discharge increases and channel bed getting steeper in the experiments including subcritical and supercritical flow conditions. However, it can be seen that the effects of walls are very high at low Froude numbers. In general, the results indicate that the perturbations in the distribution of local friction factor are quite considerable in steeper channels as Froude number increases.

Keywords V-Shaped Channel, 2D Isovels, Depth-Averaged Velocity, Boundary Shear Stress, Local Friction Factor

چکیده در این مقاله، تحقیقات آزمایشگاهی روی توزیع ضریب اصطکاک موضعی f_b و ضریب اصطکاک کلی f در کانال با کف V - شکل ارایه می گردد که این نوع کانال ها در فاضلاب روها و زیرگذرها (کالورت ها) ظاهر می شوند. با بهره گیری از اندازه گیری های سرعت و تنش برشی می توان پیدا نمود که ضریب اصطکاک داری - ویسباخ f نسبت به سایر ضرایب مقاومت جریان از قبیل n مانینگ بسیار حساس است. توزیع های عرضی منحنی های متوسط عمقی سرعت و تنش برشی جداره در مقطع کانال با شرایط مختلف جریان ارایه می شود. داده های آزمایشگاهی حاصل از اندازه گیری تنش برشی جداره τ_b و سرعت متوسط عمقی U_d برای برآورد f_b استفاده می شود. نتایج نشان می دهد که ضریب اصطکاک تابعی از عدد فرود جریان Fr است. آنگاه، ضریب اصطکاک موضعی در مقطع کانال ثابت باقی نمی ماند. در عین حال، فرض ثابت بودن ضریب اصطکاک در کل مقطع به عنوان یک فرضیه ی نظری می باشد. نتایج نشان می دهد که ضریب اصطکاک کلی مقطع با افزایش دبی جریان و تندتر شدن شیب طولی کانال در شرایط جریان های زیربحرانی و فوق بحرانی کاهش می یابد. با این حال ملاحظه می شود که در اعداد فرود پایین تر، تأثیر دیواره یا جداره زیاد است. به طور کلی نتایج نشان می دهد که برجستگی ها و بی نظمی ها در نمودارهای توزیع ضریب اصطکاک موضعی به ویژه در کانال های با شیب تند که عدد فرود جریان بالاست، قابل ملاحظه است.

1. INTRODUCTION

The relationship between flow characteristics and resistance coefficients has been well documented, in the past literatures. After Darcy-Weisbach and Prandtl and von Karman, a large number of papers have been published on flow through pipes and

open channels with smooth and rough boundaries for example, see [1-8] and elsewhere. The need for a formula on which the design of conduits and open channel flow could be based on, was recognized as early as the eighteenth century. Purely empirical methods, which provided an approximate solution for many years, have

gradually given way to attempts at a fundamental physical explanation of flow resistance [9]. A review of previous studies on the effects of shape on resistance to flow in a smooth open channel together with some especial analysis and comments are given in [10-12]. It has long been acknowledged that the variation of friction factor with Reynolds number, Re , for open channel flow is larger than smooth pipe flow at the same value of Re number. The larger friction factor is clearly due to the effects of cross sectional shape. According to Shih, et al [13] mild slope channels give less resistance to flow, than the steeper ones. Furthermore, Powell, et al [14] states that for the case of supercritical flows, the resistance follows a somewhat different law.

The influence that the free surface exerts on the resistance parameters has also been examined by a number of researchers e.g. [15-26] and especially for a V-shaped bottom channel (Figure 1), see [27-29] to name but a few. The increase in numerical modelling in the last decade has augmented the need for good quality experimental data, and has also highlighted that the local resistance parameters are as important to the numerical modeler as the global values are to engineers.

Turbulent uniform flow characteristics in a straight channel with V-shaped bottom have been experimentally investigated. This paper seeks to examine local and global friction coefficients in a V-shaped bottom channel; a cross-section which frequently occurs in many sewers, culverts and bridge/road drainage channels. Experimental results are presented concerning the boundary shear stress and depth-averaged velocity distributions across the channel section. In order to explore the

flow behavior, the local boundary shear stress measured around the perimeter. In order to establish the isovel patterns, a fictitious grid comprising of 10×10 mm squares was placed over the cross section and point velocity figures were measured. The lateral distribution of local boundary shear stress and depth-averaged velocity for both mild and steep slope channels are presented. Using both boundary shear stress and local depth-averaged velocity it is possible to evaluate the depth mean friction factor at various transverse distances across the channel bed. For both velocity and boundary shear stress, the data are analyzed from a variety of different perspectives, and the results from each analysis are used to interpret the mechanics occurring in the flow [29]. The findings from each perspective complement each other and highlight the consistency of the experimental data. The information in this paper may prove useful to any computational modelers dealing with channels of a similar cross section. The work may also be valuable to environment engineers trying to solve sludge transport problem in sewers and culverts.

2. EXPERIMENTAL APPARATUS AND PROCEDURE

To investigate the hydraulic characteristics of a V-shaped bottom channel, several series of experiments were conducted for measuring point velocity and boundary shear stress. The described experimental channel built inside the existing 15m long tilting flume. Low and high speed velocity

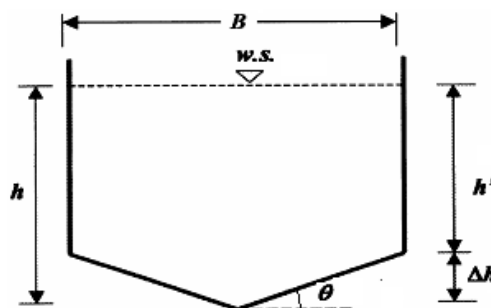


Figure 1. A V-shaped bottom channel cross-section.

propellers were used for measuring point velocities, and a Preston tube was used to measure dynamic pressures to evaluate the boundary shear stress. For a certain channel bed slope, a discharge was introduced and uniform flow was established using stage-discharge results and discharge-tailgate relationships. The flume was supported by two hydraulic jacks and rotated about a hinge joint beneath the middle of the channel. The flume also had a motorized slope control system with a mechanical visual read out on a ruler at the upstream end of the flume used for determining the precise channel bed slope. The maximum slope obtainable was $S_0 = 2\%$. The experimental channels, with a V-shaped bottom cross section built by using PVC panels to make a 14.5 m long channel having 50 mm cross fall, were built along the inside centerline of the existing flume.

Water was supplied to the channel by an overhead tank through a 101.6 mm pipeline for discharges up to 30 l/s and a 355.6 mm pipeline for discharges higher than 30 l/s. To reduce large-scale disturbance, and in order to ensure that the flow was uniformly distributed, a system of honeycombing was placed at the upstream end of the channel where the entrance tank and bell-mouth shaped inlet transition section were located. However for the case of supercritical flow i.e. $Fr > 1$ the honeycomb was not very useful. Individual bell-mouth shaped transition sections were designed and made for each channel types and served to reduce separation and improve the development of the mean flow into the channels. An electromagnetic flow meter was installed in the supply line and was used to measure discharges. The flume has a very rigid bottom designed for high loads, and therefore it was not necessary to do any deflection tests.

A slatted tailgate weir was installed in the downstream end of the channel in order to minimize upstream disturbance of the flow, and hence allowed a greater reach of the channel to be employed for experimental measurement in subcritical flows. The test section consisted 12 m long zone, commencing at a distance of 1.25 m from the channel entrance and 1.85 m from the flume entrance. However, for supercritical flows, because of the S2 profiles, the test length was reduced to about 7 m. A trolley was mounted on rails running along the flume with a depth probe,

having an electrical contact to the water surface level (accurate to 0.1 mm) and hence the channel bed slope was obtained. It has also been possible to do lateral measurements using the same trolley. The depth was measured at one meter and sometimes half a meter intervals in the test length by means of a centerline pointer probe moved down from the instrument carriage.

Point velocity was measured at different transverse locations over the channel cross-section using low and high speed propellers. For every set of flows both point velocities in cross section and dynamic pressures, in contact with channel boundary were measured for the same flow condition.

The present research work also deals with the boundary shear stress measured around the wet perimeter. Local boundary shear stress was measured using the Preston tube technique with a probe having $d = 4.705$ mm outer diameter. The tube was mounted on a carriage and aligned vertically near the walls and normal to the bed. It was also placed on the channel boundary every 10 mm intervals on the vertical walls and every 20 mm intervals on the bed in the spanwise direction. The total pressure arising from the difference between the static and dynamic pressures were recorded by connecting the tube to a simple manometer inclined at 12.52° to the horizontal. The static pressure was measured separately using a Pitot static tube at the centerline of the measuring section, and should allow at least 5 minutes to achieve an accurate reading. By 1965 Patel [31] calibrated a set of experiments using three different pipes and 14 Preston tubes. He developed the two dimensionless parameters given by:

$$x^* = \text{Log} \left(\frac{\Delta P d^2}{4 \rho v^2} \right); \text{ and } z^* = \text{Log} \left(\frac{\tau \cdot d^2}{4 \rho v^2} \right) \quad (1)$$

where,

$$z^* < 1.5 \quad z^* = 0.5x^* + 0.037 \quad (2a)$$

$$1.5 < z^* < 3.5$$

$$z^* = -0.006x^*{}^3 + 0.1437x^*{}^2 - 0.1381x^* + 0.8287 \quad (2b)$$

$$z^* > 3.5 \quad x^* = z^* + 2 \text{Log} (1.95z^* + 4.10) \quad (2c)$$

Using Equation 1 the local bed shear stress, τ , is evaluated.

3. MEAN FLOW STRUCTURE

It is difficult to examine boundary shear stress without recourse to the distribution of local

velocity within the channel. Figure 2 illustrates an example of the isovel patterns for a V-shaped channel for $Q = 85.32$ l/s at $S_0 = 0.004$. The isovel patterns demonstrate that the steep velocity gradients occur close to the bed and walls that are one of the characteristics of turbulent flow. From the other isovel plots (not shown here), it may be found that, as the flow depth increases, the isovels become more distorted and the flow becomes 3-

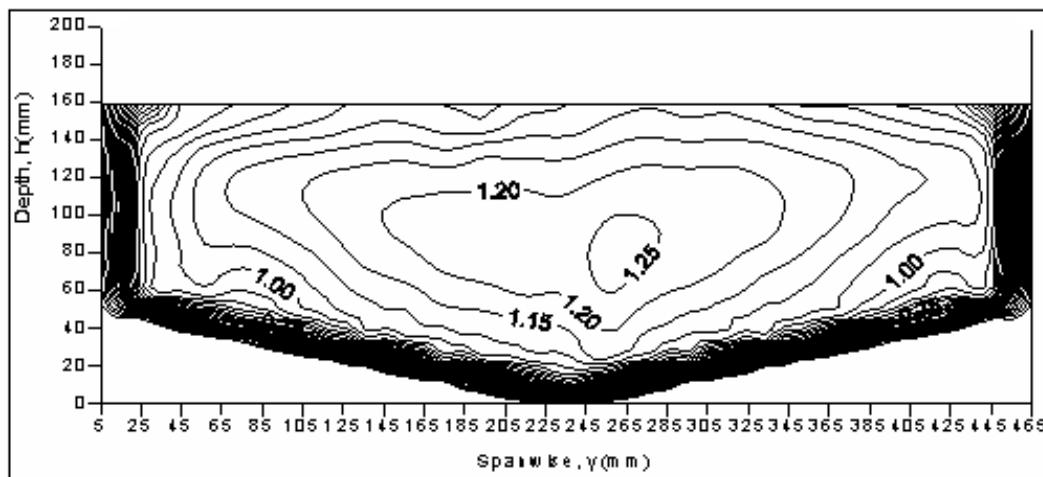


Figure 2. Isovels (u/U) in a V-shaped bottom channel, $Q = 85.32$ l/s, $S_0 = 0.004$ and $U = 1.39$ m/s.

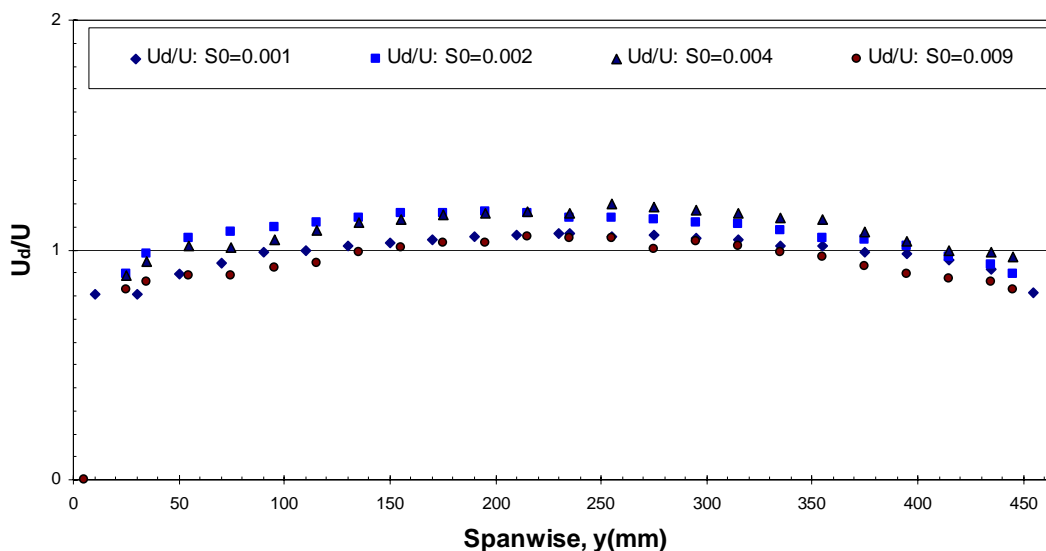


Figure 3. Lateral distribution of normalized depth-averaged velocity, U_d/U in a V-shaped channel: $Q = 85$ l/s.

dimensional across the whole cross-section. As the flow becomes more 3-dimensional, the position at which the maximum velocity occurs is depressed further below the water surface [29,30]. The local velocity was measured at each node of the grid, using propellers as explained in previous section. To check the discharges, the mean velocity of a sub area formed by the grid, was assumed to be equal to the average of the four point velocities at the corresponding nodes. Multiplying the small sub area by its local average velocity allowed, the discharge corresponding to the sub area to be evaluated. Numerically integrating the discharges in each of the small sub areas allowed the total discharge across the channel to be evaluated. Due to the curvature of the wall, near the channel boundaries, it was necessary to approximate some of the sub areas formed by the grid. This value was then compared to the true discharge obtained from a calibrated electromagnet flowmeter.

4. LATERAL BOUNDARY SHEAR STRESS, τ_b , AND DEPTH-AVERAGED VELOCITY, U_d

Using the local velocity it is possible to evaluate the depth-averaged velocity at various transverse distances across the channel bed. Integrating the local velocities, u , over the flow depth, h , gives the depth-averaged velocity, U_d . The depth-averaged velocity was converted to a dimensionless parameter by use of the section mean velocity, U ($= Q/A$). As an example, Figure 3 shows the lateral variations of depth-averaged velocities and also their normalized distributions for different flow discharge and slope settings. The section mean velocities are also shown as solid lines related to every flow test on the same figures. It can be seen from these figures that the distributions are almost symmetrical about the cross sectional centerline, but they deviate for some flow cases despite the flow condition was uniform for all cases. At large flow depths of the maximum velocity occurs at the centerline and reduces continuously towards the sidewalls indicating that the sidewalls exert a large influence on flow behavior. Figures likewise Figure 3 also illustrates that there appears to be very little noticeable difference in the flow

structure between subcritical and supercritical flows. The slight difference is manifested by the depth-averaged velocity for supercritical flow being slightly larger than the corresponding value for subcritical flow.

Analysis of the boundary shear stress distributions illustrated that there is a slight Froude number effect [29]. A typical distribution of boundary shear stress is shown in Figure 4, where the local data have been adjusted by the global value ($= \rho g R_h S_f$) and the perimetric distance refers to the transverse distance around the wet perimeter divided by the total wet perimeter. The large variation in boundary shear stress highlights the complex flow patterns occurring at this flow depth. This is because of the effect of channels' cross sectional shape and the presence of secondary currents at the higher flow depths in steep slopes where Fr number increases. As previously mentioned the analysis of flow patterns or boundary shear stress is a difficult problem. In order to overcome this recourse is often made to a resistance coefficient, usually the Darcy-Weisbach friction factor, f , or Manning's coefficient, n . Both of the coefficients are explained in next section. These data would be useful for validating various computational models, such as the 2D depth-averaged model given by Shiono, et al [32] and Wilkerson, et al [33]. It can be seen from this figure that some deviations are observable. This leads to the view that the secondary current cells affect the flow behavior.

5. GLOBAL FRICTION FACTOR

The global friction factor, f , follows the trend of the smooth law given by the following (so-called Karman-Prandtl equation):

$$\frac{1}{\sqrt{f}} = -2 \log \left(\frac{2.51}{Re \sqrt{f}} \right) \quad (3)$$

The experimental global friction factors were evaluated from the stage-discharge relationships using Equation 3. Figure 5 illustrates the variation of f with Reynolds number, Re , for both subcritical and supercritical flow conditions. From Figure 5, it appears that the trend for the $S_0 = 0.001$ data is to

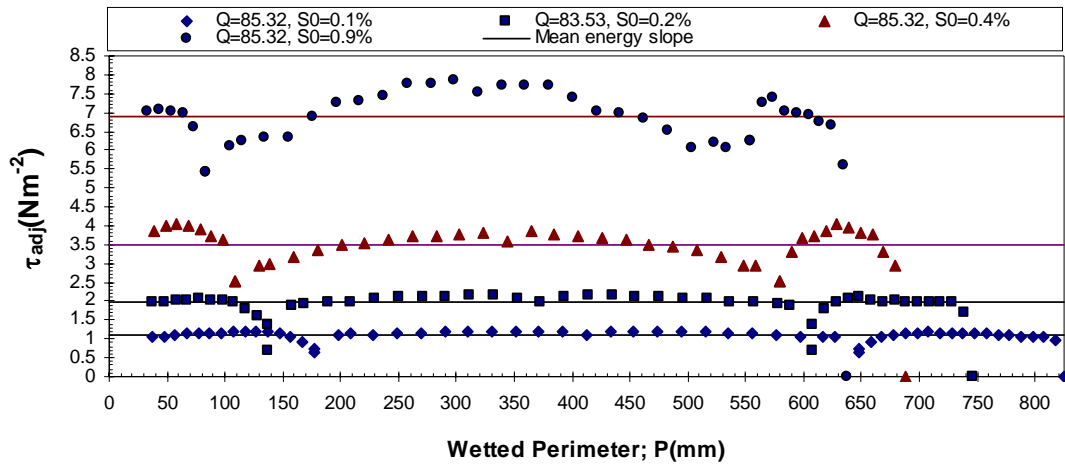


Figure 4. Lateral distribution of boundary shear stress, τ_b , adjusted to the mean energy slope value ($= \rho g R S_0$): $Q = 85$ l/s.

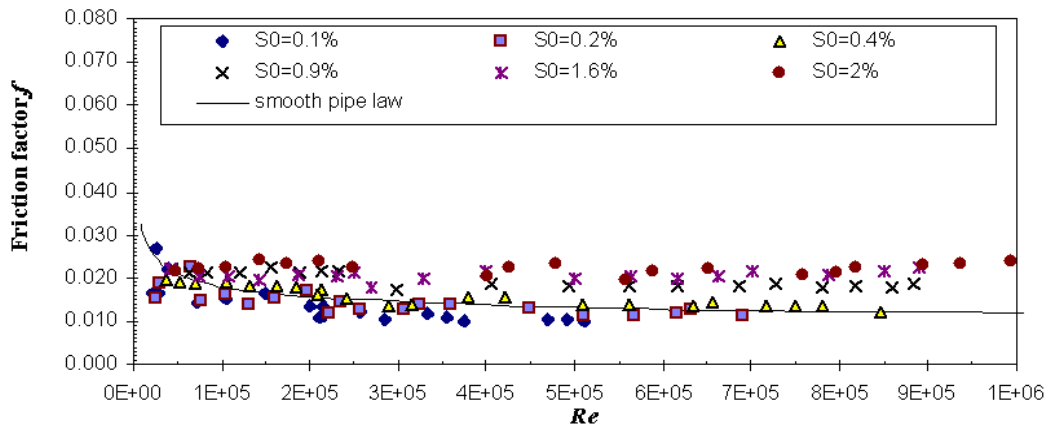


Figure 5. Friction factor, f , versus re number.

cross the smooth law. As the Reynolds number, Re , increases the stage also increases, (for a constant channel bed slope). The increase in stage increases the difficulty in setting M1 and M2 water surface profiles and as a consequence in establishing a normal flow depth. Hence the pronounced scatter at high Re number is more indicative of experimental technique rather than any hydraulic phenomenon.

Figure 5 (and other data given by Mohammadi [27]) illustrates that the global resistance for

supercritical flow is greater than subcritical flow, (for the current range of Reynolds numbers examined). What is noticeable from Figure 5 is that a small reduction in flow depth results in a large increase in friction factor. Although this increase can also be obtained from the Moody-Stanton diagram, over certain low Reynolds numbers, this does not explain the large increase in local friction factor at small depths of flow. According to Shih, et al [13] mild slope channels give less resistance to flow than the steeper ones.

Furthermore, Powell, et al [14] states that for the case of supercritical flows, the resistance follows a somewhat different law.

It is common-place to analyze the resistance to flow in open channels in terms of Manning's n . However, as Darcy-Weisbach f is more sensitive than Manning's n , this may qualify to use f rather than n for some means in open channels resistance calculations. Manning's n is related to the friction factor, f , (see [7,28]) as follow:

$$n = \sqrt{\frac{f}{8g}} R^{1/6} \quad (4)$$

Where R is the hydraulic radius of the channel. Figure 6 shows the variation of n verses flow discharge. Again the dependency of resistance coefficient with Froude number is noticeable, however, n appears to be independent of the depth of flow discharge. As a consequence of the reduction in Reynolds number the depth of flow is also reduced, (for a constant bed slope). As a consequence of the decrease in stage the hydraulic radius decreases, hence the relative roughness ($k_s/4R$) increases (see Mohammadi [10]). The increase in relative roughness is manifested by an increase in local friction factor. This phenomenon has been noted previously by Knight, et al [34] who found that at low depths of flow, (and low Reynolds number) the magnitude of the Nikuradse k_s increased beyond the actual flow depth. Although the overall resistance of a channel is of

great importance, it is often useful to know and understand the variation of local resistance coefficient.

6. LOCAL FRICTION FACTOR

In open channel flows, the estimation of local friction factor is one of the more important tasks and sometimes a very difficult one. This difficulty arises from the existence of the secondary flow cells and the boundary induced turbulence, both of which affect the distributions of depth-averaged velocity and boundary shear stress, and consequently the local friction factor. Using the measured local depth-averaged velocity, U_d , and the local bed shear stress, τ_b , the local depth-averaged bed friction factor, f_b , was calculated for each lateral position by applying (Shiono, et al 2D model [32]) as:

$$f = \frac{8\tau_b}{\rho U_d^2} \quad (5)$$

As an example, the lateral distribution of local depth-averaged friction factor is shown plotted in Figure 7 for $Q = 10$ l/s at different channel bed slopes. As can be seen from this figure, the distributions are close together for low flow discharges in both subcritical and supercritical flow conditions, but there are more variable for the

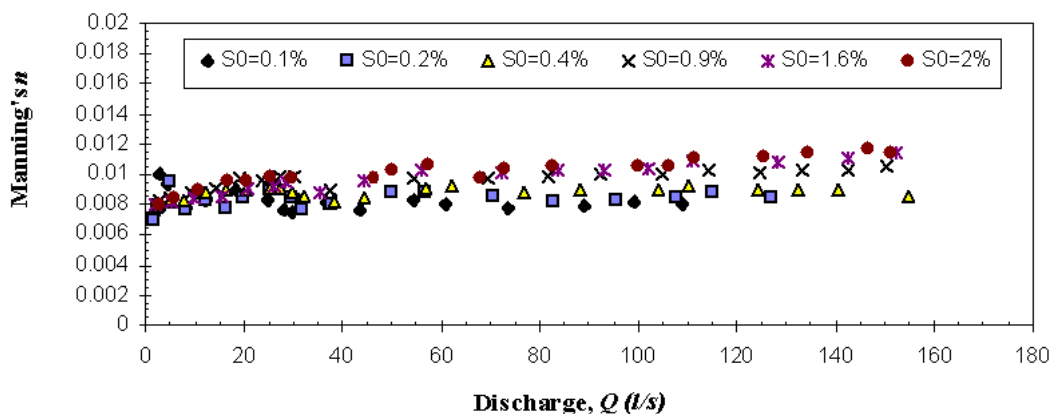


Figure 6. Manning's n versus flow discharge, Q .

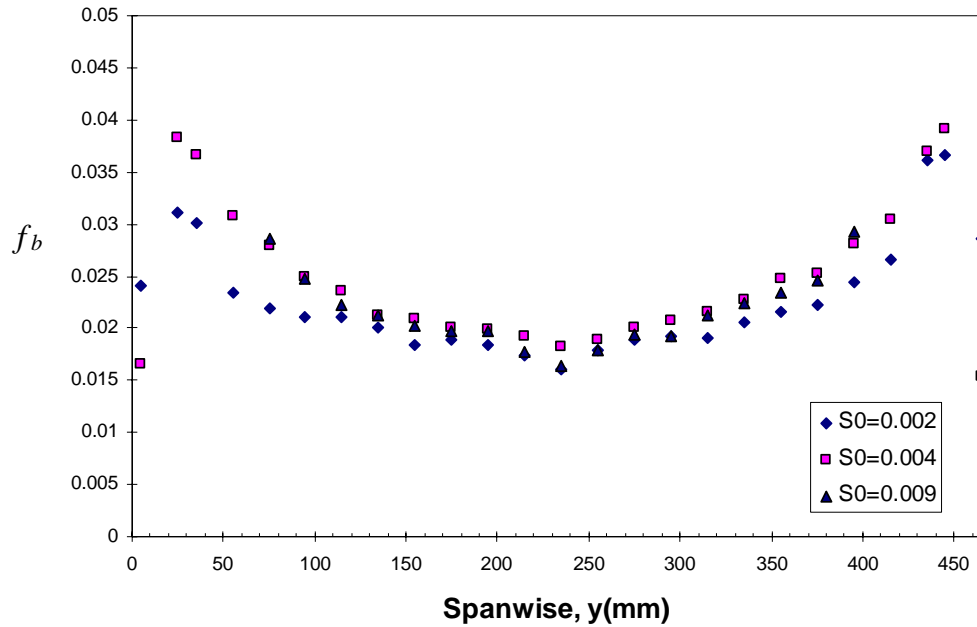


Figure 7. Lateral distribution of depth-averaged friction factors: $Q = 10$ l/s.

higher flow discharges (see Mohammadi [27]). The local friction factor results were then normalized to the global friction factor, f , value. The normalized local friction factors, f_b/f , are shown plotted in Figures 8a-d. It can be seen from these figures that the discrepancy in the higher flow rates are larger than that of the lower flow rates. More importantly the figures show that the local f values tend towards a more constant distribution at high flow discharges than low flow discharges. Figures 8a-d illustrate that, despite the wide range of flow conditions investigated, the local friction factor remains almost constant across a large proportion of the channel bed, despite the large variations in τ_b and U_d . This indicates that the local boundary shear stress is directly proportional to the square of the depth-averaged velocity across a large proportion of the bed. The dramatic increase in local friction factor at the extreme edges of the channel bed is due to the depth averaged velocity decreasing at a faster rate than the local boundary shear stress.

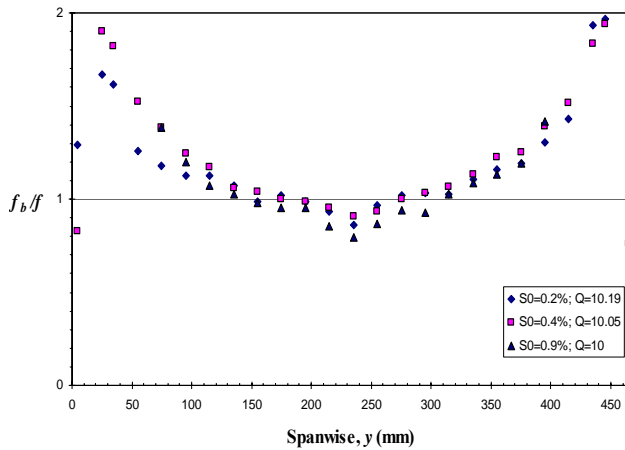
In many situations it is favorable to be able to quantify the local resistance of boundary elements, e.g. in the field of sediment transport (see [35,36]) The elements of the boundary under consideration

are often classified as either the bed or walls of the channel. The method used for calculating the friction factor which embodies the influence of the wall, (or bed) is often referred to as the side wall correction procedure (see Mohammadi [27] and Sterling [36]).

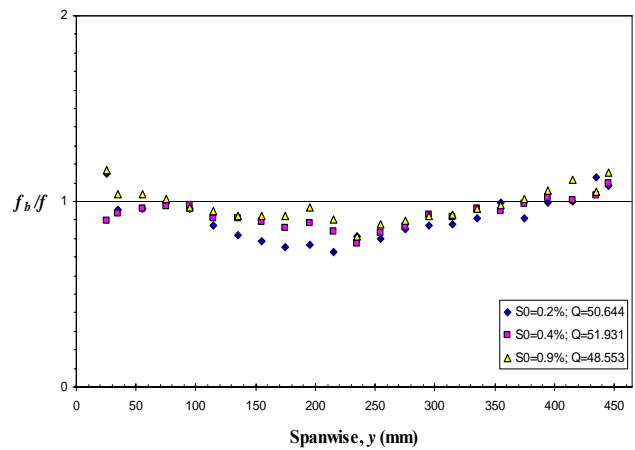
7. CONCLUDING REMARKS

In this paper the results on velocity, boundary shear stress and local friction factor for a fully developed turbulent flow are presented. It has also examined certain aspects of the flow which combines to contribute, to the local and global resistance coefficients of a channel. On the basis of the results already presented in earlier sections, the major results and findings are as follows:

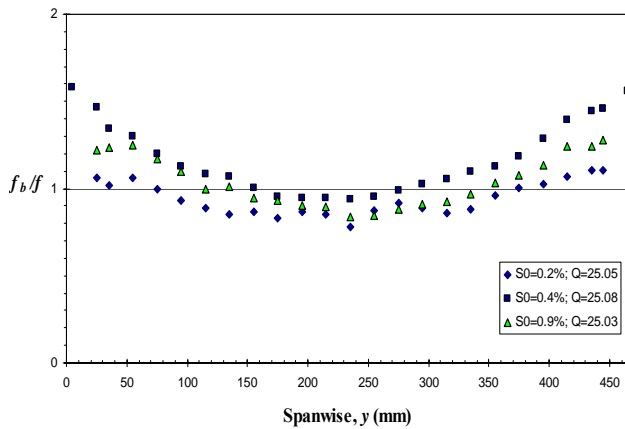
- A range of target flow discharges, i.e. 10, 25, 50 and 85 l s^{-1} , at four channel bed slopes of 0.001, 0.002, 0.004 and 0.009, is examined. Hence, the ranges of Re and Fr numbers are: $2.332 \times 10^4 < Re < 1.82 \times 10^5$ and $0.539 < Fr < 2.27$, respectively.



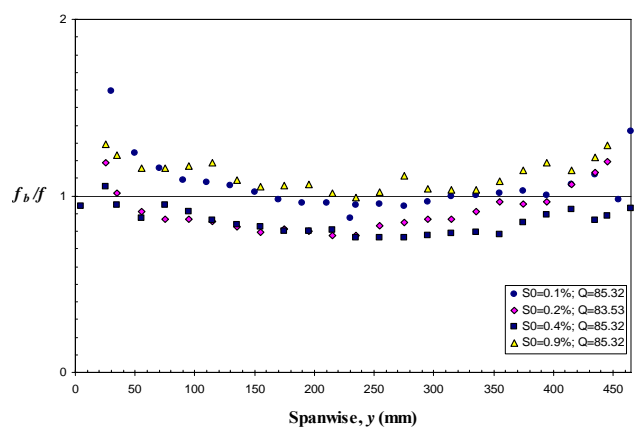
(a)



(b)



(c)



(d)

Figure 8. Lateral distribution of normalized local friction factor, f_b/f ,
(a) $Q = 10$ l/s, (b) $Q = 25$ l/s, (c) $Q = 50$ l/s, (d) $Q = 85$ l/s.

- It appears from the boundary shear stress results, that the lateral distributions are very flat at low Froude numbers. Thus for a certain flow discharge the active width decreases as the Fr number increases (i.e. the channel gets steeper).
- The isovel plots are generally symmetric, except in the central region where a local maximum occurs. However, it seems that the generally symmetrical distributions of primary flow are sometimes unstable, so that an alternative pattern of asymmetry may

form. Such an alternating pattern is random for different flow conditions, being affected by secondary flow cells which make the flow 3D.

- The resistance relationship for such a complicated channel cross section is more complex than that of simple rectangular or trapezoidal shape channel. This may indicate the presence of other variables, related to the influence of secondary currents and the importance of internal shear and momentum transfer mechanisms.

- The flow resistance appears to increase as the channel bed slope becomes steeper. The results clearly show that for a certain Reynolds number the resistance is higher than that of the Prandtl smooth pipe law for supercritical flows i.e. $Fr > 1$, and it gives less resistance than the smooth pipe law for subcritical flows, i.e. $Fr < 1$. This is the case either for the Manning n or for the Darcy-Weisbach, f . The same pattern was obtained for the variation of friction factor with aspect ratio, B/h .
- The resistance analysis indicates that the Darcy-Weisbach, f , is a more sensitive parameter than the Manning n and has been shown to vary with depth. However, those resistance parameters are little dependent on the channel bed slope, i.e. the resistance increases as the channel gets steeper, and the trends increase systematically from mild slope to steep ones.
- The resistance processes of flow can be described as a function of Reynolds number, Re , Froude number, Fr , and channel geometry. Full mathematical quantification of the function is not yet possible, but semi-empirical analysis using extensive flume data supports the theory and has allowed the development of a basic theoretical resistance equation. Development of a more general equation depends on detailed studies of individual processes for different channel cross sections over a large range of either Reynolds, Re , or Froude, Fr , numbers.
- The local friction factor remains constant across the channel despite the large variations in boundary shear stress and the accuracy of depth-averaged velocity occur.
- The dramatic increase in local friction factor, f , at the extreme edges of the channel bed is due to the depth averaged velocity decreasing at a faster rate than the local boundary shear stress.
- Figure discrepancies in the higher flow rates are larger than that of the lower flow rates. More importantly the figures show that the local friction factor, f , values tend towards a more constant distribution at high flow discharges than low flow discharges.

8. ACKNOWLEDGEMENT

The author would like to express his sincere thanks to the University of Urmia for providing research expenses.

9. NOMENCLATURE

A	Transverse Cross-Sectional Area;
B	Top Width or Breadth of Channel;
d	Pitot Tube Outer Diameter;
f	Darcy-Weisbach friction factor;
f_b	Local Friction Factor;
Fr	Froude Number ($= U/\sqrt{gA/B}$);
g	Acceleration due to the Gravity;
h	Flow Depth;
h_f	Friction Head Loss;
k_s	Nikuradse Resistance Coefficient;
n	Manning's Roughness Coefficient;
Q	Flow Discharge;
R	Hydraulic Radius ($= A/P$);
Re	Reynolds Number ($= 4UR/\nu$);
s	Side Channel Slope;
S_0	Channel Bed Slope;
S_e	Longitudinal Energy Slope;
S_f	Friction Slope;
U	Mean Velocity in the Direction, x;
U_d	Depth-Averaged Velocity;
x	Streamwise Co-Ordinate;
y	Transverse Co-Ordinate;
z	Vertical Co-Ordinate;
x^*, z^*	Calculation Parameters in Patel's Calibration;
θ	Acute Angle Between Bottom Parts of Channel and Horizontal Line;
ρ	Fluid Density;
ν	Fluid Viscosity;
ΔP	Pressures Difference Due Dynamic and Static Pressures;
τ	Shear Stress;
τ_b	Boundary Shear Stress;

10. REFERENCES

1. Nikuradse, J., "Stromungsgesetze in Rauhen Rohren", Forschungsheft, Verein Deutscher Ingenieure, (Translated

- into English as NACA TM 1292), Berlin, Germany, No. 361, (November 1950).
2. Colebrook, C. F. and White, C. M., "Experiments with Fluid Friction in Roughened Pipes", *Proc. Roy. Soc.*, Vol. 161, (1937), 367-381.
 3. Keulegan, G. H., "Laws of Turbulent Flow in Open Channels, *Journal of Research of the National Bureau of Standards*, Research Paper 1151, Washington DC, U.S.A., Vol. 21, (December 1938), 707-741.
 4. Moody L. F., "Friction Factor for Pipe Flows", *Trans. Am. Soc. Mech. Engrs*, Vol. 66, (1944), 671.
 5. ASCE Task Force of Hydrodynamics Committee, "Friction Factors in Open Channels: Progress Report of the Task Force on Friction factors in Open Channels of the Committee", *Journal of Hydr. Div., ASCE*, Vol. 89, HY2, (March 1963), 97-143.
 6. Rouse, H., "Critical Analysis of Open Channel Resistance, *J. Hydraulics Div., ASCE*, Vol. 91, HY4, (July 1965), 1-25.
 7. Yen, B. C., "Hydraulic Resistance in Open Channels, in Channel Flow Resistance: Centennial of Manning's Formula", *Water Resources Publication*, (Yen, B. C., Edited), Colorado, U.S.A., (1992), 1-136.
 8. Pillai, N. N., "Effect of Shape on Uniform Flow through Smooth Rectangular Open Channels", *J. Hydraulic Eng., ASCE*, Vol. 123, No. 7, (July 1997), 656-658.
 9. Ackers, P., "The Hydraulic Resistance of Drainage Channels", HRS, Thomas Telford Journals, ICE, London, (July 1961), 307-336.
 10. Mohammadi, M., "On the Effect of Shape on Resistance to Flow in Open Channels", *Proceeding International Conference on: Fluvial Hydraulics (Riverflow2002)*, Louvain-La-Neuve, Belgium, (September 3-6 2002a), 339-348.
 11. Mohammadi, M., "Boundary Shear Stress Distribution in Open Channels having Different Cross Sections", A Research Report Submitted to the Research and Technology Department of Urmia University, Urmia, Iran, (2002b).
 12. Mohammadi, M., "Boundary Shear Stress Around Bridge Piers", *American Journal of Applied Sciences (AJAS)*, Science Publications, U.S.A., Vol. 5, No. 11, (2008), 1546-1550.
 13. Shih, C. C. and Grigg, N. L., "A Reconsideration of the Hydraulic Radius as a Geometric Quantity in Open Channel Hydraulics, *Proc. 12th Congress, IAHR*, Vol. 1, Paper A36, (September 1967), 281-288.
 14. Powell, R. W., "Resistance to Flow in Rough Channels", *Transactions, AGU*, Vol. 31 No. 4, (1950), 575-582.
 15. Jayaraman V. V., "Resistance Studies on Smooth Open Channels", *J. Hyd. Div, Proc. ASCE*, Vol. 96. No. HY5, (1970), 1129-1142.
 16. Kazempour, A. K. and Apelt, C. J., "Shape Effects on Resistance to Uniform Flow in Open Channels, *J. of Hydr. Research, IAHR*, (January 1979), 129-147.
 17. Kazempour, A. K. and Apelt, C. J., "Shape Effects on Resistance to Flow in Smooth Rectangular Channels", Dept. of Civil Eng., Research Report Series No. CE9, April, University of Queensland, Australia, (1980).
 18. Kazempour, A. K. and Apelt, C. J., "New Data on Shape Effects in Smooth Rectangular Channels", *J. Hydraulic Research, IAHR*, Vol. 20, No. 3, (March 1982).
 19. Myers, W. R. C., "Flow Resistance in Wide Rectangular Channels", *J. Hydraulics Div., ASCE*, HY4, (1982), 471-482.
 20. Nalluri, C. and Adepoju, B. A., "Shape Effects on Resistance to Flow in Smooth Channels of Circular Cross-Section", *J. of Hydraulic Research*, Vol. 23, No. 1, (1985), 37-46.
 21. Hooхло, C., "A Numerical and Experimental Study of Open Channel Flow in a Pipe of Circular cross-section With a Flat Bed", PhD Thesis, University of Newcastle Upon-Tyne, Civil Eng. Dept., U.K., (November 1994).
 22. Sterling, M. and Knight, D. W., "Resistance and Boundary Shear in Circular Conduits with flat beds Running Part full", *Proc. Instn. Civ. Engrs Water and Mar. Engng*, Vol. 142, (December 2000), 229-240.
 23. Knight, D. W. and Brown, F. A., "Resistance Studies of Overbank Flow in Rivers with Sediment using the Flood Channel Facility, *J. of Hydraulic Research, IAHR*, Vol. 39, No. 3, (March 2001), 283-302.
 24. Beecham, S., Khiadani, M. H. and Kandasamy, J., "Friction Factors for Spatially Varied Flow with Increasing Discharge", *J. Hydr. Engrg.*, Vol. 131, (September 2005), 792-799.
 25. Knight, D. W., Yuen, K. W. H. and Al-Hamid, A. A. I., "Boundary Shear Stress Distribution in Open Channel Flow", *Mixing and transport in the Environment*, (Eds: Beven, K., Chatwin, P. and Millbank, J.), John Wiley and Sons Ltd, Chapter 4, (1994), 51-87.
 26. Knight, D. W., Omran, M. and Tang, X., "Modeling Depth-averaged Velocity and Boundary Shear in Trapezoidal Channels with Secondary Flows", *J. Hydraulic Engineering*, Vol. 133, Issue 1, (2007), 39-47.
 27. Mohammadi, M., "Resistance to Flow and the Influence of Boundary Shear Stress on Sediment Transport in Smooth Rigid Boundary Channels; PhD Thesis, School of Civil Engineering, Birmingham University, England, U.K., (1998).
 28. Mohammadi, M., "Shape Effects on Resistance to Flow in a V-Shaped Channel", *Proceedings International Journal of Engineering, A Center for Scientific Research*, Tehran, Iran, Vol. 17, No. 4, (June 2005), 349-357.
 29. Mohammadi, M. and Knight, D. W., "Boundary Shear Stress Distribution in a V-shaped Channel", *Proceedings First International Conference on: Hydraulics of Dams and River Structures, (HDRS)*, Esteghlal Hotel, Tehran, Iran, <http://hdrs.pwit.ac.ir/>, (April 26-28, 2004), 401-410.
 30. Mohammadi, M., "Boundary Shear Stress Distribution in a Part-full Pipe Channels", *Proceeding 6th National Conference on: Hydraulics, Iranian Association of Hydraulics (IAH)*, University of ShahrKord, ShahrKord, Iran, (September 3-5, 2007), (in Farsi).
 31. Patel, V. C., "Calibration of the Preston Tube and Limitations on Its Use in Pressure Gradients, *J. Fluid Mechanics*, Vol. 23, (1965), 185-208.
 32. Shiono, K. and Knight, D. W., "Turbulent Open

- Channel Flows with Variable Depth across the Channel”, *J. Fluid Mechanics*, Vol. 222, (1991), 617-646.
33. Wilkerson, G. V. and McGahan, J. L., “Depth-averaged Velocity Distribution in Straight Trapezoidal Channels”, *J. of Hydr. Engrg.*, Vol. 131, Issue 6, (June 2005), 509-512.
 34. Knight, D. W. and Macdonald, J. A., “Hydraulic Resistance of Artificial Strip Roughness”, *J. of Hydraulics Division, ASCE*, Vol. 105, No. HY6, (1979), 675-690.
 35. El-Zaemey, A. K. S., “Sediment Transport Over Deposited Beds in Sewers”, PhD Thesis, University of Newcastle Upon Tyne, England, U.K., (1991).
 36. Sterling, M., “The Distribution of Boundary Shear Stress in an Open Channel Circular Conduit Running Part-Full”, PhD Thesis, University of Birmingham, Birmingham, England, U.K., (1997).